

Hemp Waste Stream Valorization Through Pyrolytic Carbonization for Epoxy Composite Strengthening

*Original*

Hemp Waste Stream Valorization Through Pyrolytic Carbonization for Epoxy Composite Strengthening / Zecchi, Silvia; Cristoforo, Giovanni; Bartoli, Mattia; Rosso, Carlo; Tagliaferro, Alberto. - In: JOURNAL OF COMPOSITES SCIENCE. - ISSN 2504-477X. - 8:11(2024). [10.3390/jcs8110473]

*Availability:*

This version is available at: 11583/2995992 since: 2024-12-28T10:53:06Z

*Publisher:*

MDPI

*Published*

DOI:10.3390/jcs8110473

*Terms of use:*

This article is made available under terms and conditions as specified in the corresponding bibliographic description in the repository

*Publisher copyright*

(Article begins on next page)



Article

# Hemp Waste Stream Valorization Through Pyrolytic Carbonization for Epoxy Composite Strengthening

Silvia Zecchi <sup>1,2,\*</sup>, Giovanni Cristoforo <sup>1</sup>, Mattia Bartoli <sup>2,3,\*</sup>, Carlo Rosso <sup>4</sup> and Alberto Tagliaferro <sup>1,2,5</sup>

<sup>1</sup> Department of Applied Science and Technology, Polytechnic University of Turin, Corso Duca degli Abruzzi 24, 10129 Turin, Italy; giovanni.cristoforo@polito.it (G.C.); alberto.tagliaferro@polito.it (A.T.)

<sup>2</sup> Consorzio Interuniversitario Nazionale per la Scienza e Tecnologia dei Materiali (INSTM), Via Giuseppe Giusti 9, 50121 Florence, Italy

<sup>3</sup> Center for Sustainable Future, Italian Institute of Technology, Via Livorno 60, 10144 Turin, Italy

<sup>4</sup> Department of Mechanical and Aerospace Engineering, Polytechnic University of Turin, Corso Duca degli Abruzzi 24, 10129 Turin, Italy; carlo.rosso@polito.it

<sup>5</sup> Faculty of Science, OntarioTech University, 2000 Simcoe Street North, Oshawa, ON L1G 0C5, Canada

\* Correspondence: silvia.zecchi@polito.it (S.Z.); mattia.bartoli@iit.it (M.B.); Tel.: +39-3348574791 (S.Z.)

**Abstract:** This research addresses a gap in the literature by exploring the combined use of hemp and hemp hurds in composites, presenting a novel approach to bio-composite development. We report on the mechanical properties of epoxy resin composites reinforced with hemp fibers and hemp hurds, selected for their sustainability, biodegradability, and environmental benefits. These natural fibers offer a renewable alternative to synthetic fibers, aligning with the growing demand for eco-friendly materials in various industries. The primary objective was to evaluate how different filler contents and hemp hurd-to-hemp fiber ratios affect the composite's performance. Composites with 1:1 and 3:1 ratios were prepared at filler concentrations ranging from 1 wt.% to 10 wt.%. Tensile tests revealed that the 3:1 ratio composites exhibited better stiffness and tensile strength, with a notable UTS of  $19.8 \pm 0.4$  MPa at 10 wt.%, which represents a 160% increase over neat epoxy. The 1:1 ratio composites showed significant reductions in mechanical properties at higher filler contents due to filler agglomeration. The study concludes that a 3:1 hemp hurd-to-hemp fiber ratio optimizes mechanical properties, offering a sustainable solution for enhancing composite materials' performance in industrial applications.

**Keywords:** hemp fibers; hemp hurds; composites; mechanical properties



**Citation:** Zecchi, S.; Cristoforo, G.; Bartoli, M.; Rosso, C.; Tagliaferro, A. Hemp Waste Stream Valorization Through Pyrolytic Carbonization for Epoxy Composite Strengthening. *J. Compos. Sci.* **2024**, *8*, 473. <https://doi.org/10.3390/jcs8110473>

Academic Editors: Jeevithan Elango, Kuppusamy Kanagaraj and Natesan Thirumalaivasan

Received: 4 October 2024

Revised: 8 November 2024

Accepted: 12 November 2024

Published: 14 November 2024



**Copyright:** © 2024 by the authors. Licensee MDPI, Basel, Switzerland. This article is an open access article distributed under the terms and conditions of the Creative Commons Attribution (CC BY) license (<https://creativecommons.org/licenses/by/4.0/>).

## 1. Introduction

The development of composite materials has gained significant attention during recent years, driven by the need for sustainable and high-performance alternatives to conventional materials [1,2]. Among these, composites reinforced with natural fibers have emerged as a promising solution, due to their advantageous mechanical properties and environmental benefits [3–5]. Hemp fibers and hemp hurds are particularly attractive as reinforcements for polymer matrices, owing to their excellent strength-to-weight ratios, biodegradability, and lower environmental impact compared to synthetic fibers [6,7]. Hemp fibers stand out as the most cost-effective, widely available, and frequently used among hemp-derived products for reinforcing materials in both cementitious and polymer matrices [8,9]. Known for their high tensile strength and stiffness, hemp fibers provide significant mechanical reinforcement, while hemp hurds, being more lignified and less dense, contribute to the lightweight nature of the composites [10–12]. The incorporation of natural fillers into epoxy resin matrices not only enhances the mechanical properties of the resulting composites but also promotes sustainability by reducing reliance on non-renewable resources and decreasing carbon footprints [13–17]. Hemp-based composites provide several benefits over traditional synthetic materials, including lower embodied energy, improved acoustic

insulation, and a superior lifecycle performance [18]. These advantages are increasingly valued in industries such as construction, automotive, and packaging, where the shift toward greener materials is crucial to meet growing regulatory and consumer demands [19,20]. Recent research into natural fiber-reinforced composites highlights how hemp fibers compare favorably to other natural fibers, such as flax and jute [21,22]. The mechanical properties of hemp-reinforced composites, such as their specific modulus and toughness, position them as a viable substitute in sectors like automotive and marine industries, where weight reduction and environmental performance are critical [23]. Comparatively, biocomposites made from other natural fibers, such as flax, also perform well, but hemp has the added advantage of lower density and better availability [24]. Recent advancements in nano-enhanced composites, where nano-silica or graphene is incorporated into the epoxy matrix, have further strengthened the performance of hemp composites, making them suitable for even more demanding structural applications [25]. Despite the many advantages of hemp-based composites, challenges remain, especially regarding their behavior in harsh environmental conditions. Moisture absorption can lead to degradation of the fiber-matrix interface, reducing tensile and flexural properties [22,26–28]. However, innovative treatments and coupling agents have shown promise in improving water resistance and durability, ensuring the longevity of hemp composites in real-world applications [29,30].

However, most current studies in the literature focus on composites made with either hemp fibers or hemp hurds individually [11,31–33]. While these studies reported enhancements in specific mechanical properties, such as tensile strength and modulus, they often overlook the potential benefits of combining both fillers [34,35]. For instance, composites reinforced solely with hemp fibers exhibit high strength and stiffness but may suffer from brittleness, whereas those with only hemp hurds tend to be more ductile but may lack sufficient strength [32,36]. The limited exploration of hybrid composites that incorporate both hemp fibers and hemp hurds has left a significant gap in understanding how the synergistic effects of these fillers can optimize the mechanical performance of the materials.

This study aims to address these limitations by systematically evaluating the mechanical properties of epoxy resin composites reinforced with varying concentrations and ratios of hemp fibers and hemp hurds. Through a comprehensive analysis of the tensile strength, elastic modulus, elongation at break, and toughness, this research seeks to provide a deeper understanding of how these natural fillers influence the performance of the composites. The novelty of this work lies in its detailed investigation of the synergistic effects of hemp fibers and hemp hurds, particularly focusing on optimizing their ratio and concentration to achieve a balanced enhancement in mechanical properties. Furthermore, this study contributes to the growing body of knowledge on sustainable composite materials, offering valuable insights for future applications in industries seeking eco-friendly and high-performance materials.

## 2. Materials and Methods

### 2.1. Materials

Hemp fibers and hemp hurds were purchased from Assocanapa (Turin, Italy). Short hemp fibers were those less than 10 cm long and were not suitable for other applications. The two-component resin was purchased from CORES (Cores epoxy resin, LPL). The monomer was bisphenol-A diglycidyl ether, while the curing agent was composed of a mix of amines (1,3-phenylenedimethanamine and  $N^1,N^3$ -dimethylpropane-1,3-diamine) and 2,4,6-Tris(dimethylaminomethyl)phenol as catalyst for the polymerization [37]. The weight ratio of monomer to curing agent was 2:1.

### 2.2. Methods

#### 2.2.1. Filler Production

The hemp fibers were reduced in size in order to be more easily processed. Both hemp fibers and hemp hurds were thermally treated in a tubular furnace (Carbolite TZF 12/65/550) under a nitrogen atmosphere. This process involved a heating rate of 15 °C/min,

reaching and maintaining a temperature of 400 °C for 30 min for the hemp fibers and 550 °C for 30 min for the hemp hurds.

The treatment of hemp fibers at 400 °C and hemp hurds at 550 °C was conducted with distinct purposes aimed at enhancing the composite's mechanical performance and improving the compatibility between the natural fillers and the epoxy matrix.

For the hemp fibers, the treatment at 400 °C was necessary to remove hemicelluloses, lignin, and pectins, which are hydrophilic and contain hydroxyl (OH) and carboxylic acid groups [11]. These groups tend to absorb water, making the fibers incompatible with the nonpolar, hydrophobic nature of the epoxy matrix. The heat treatment improves the adhesion between the fiber surface and the epoxy matrix, as it reduces the presence of polar groups that otherwise weaken the fiber–matrix bond.

At 550 °C, the hurds undergo pyrolysis, which increases their stiffness and thermal stability. The resulting carbonized material becomes less reactive, with reduced moisture content and a higher surface area. This allows the hurds to act as rigid reinforcements within the epoxy matrix, contributing to improved stiffness and overall mechanical properties of the composite.

Hemp was then retrieved and utilized without undergoing any additional steps. Hemp hurds underwent pulverization using a TURBULA<sup>®</sup> mixer T 2 F (Willy A. Bachofen, Muttenz, Switzerland) for 1 h.

### 2.2.2. Composite Production

The fillers were manually mixed into the resin monomer for 10 min. After adding the curing agent, the solution was mixed again for another 2 min. The mixture was then poured into a 3D-printed PLA mold and left to cure at room temperature for 24 h. After the initial curing, the specimens were thermally cured in a ventilated oven (I.S.C.O. Srl, “The Scientific Manufacturer”, Venice, Italy) at 50 °C for 7 h. This temperature was chosen to prevent PLA degradation, avoiding mold shrinkage and specimen deformation.

To assess the impact of filler content on mechanical properties, various filler loadings were tested. Specifically, filler concentrations of 1 wt.%, 3wt.%, 5wt.%, and 10wt.% by weight were used for both filler families. For tensile and flexural tests, five samples were prepared for each concentration to ensure reproducibility and enable statistical analysis. Specimens without fillers were also produced as reference samples for mechanical characterization. Due to the different nature of the tests, multiple types of specimens were manufactured: Dog bone-shaped specimens were produced for the tensile test according to BS EN ISO 527-2:2012 [38], while bar specimens were used for the flexural test according to BS EN ISO 178:2019 [39].

### 2.2.3. Filler Precursors and Filler Characterization

The morphology of hemp and hemp hurds was observed using a field-emission scanning electron microscope (FE-SEM, Zeiss SupraTM40, Oberkochen, Germany). The instrument was equipped with an energy-dispersive X-ray detector (EDX, Oxford Inca Energy 450, Oberkochen, Germany) for compositional evaluation of the hemp hurds and hemp fibers. The Raman spectra of both powders were collected using a Renishaw InVia (H43662 model, Gloucestershire, UK) equipped with a laser line emitting at a wavelength of 514 nm and a 50× objective lens. Raman spectra were recorded in the range of 150 cm<sup>-1</sup> to 3500 cm<sup>-1</sup>, and the region between 800 cm<sup>-1</sup> and 2000 cm<sup>-1</sup> was analyzed using homemade software compiled in MATLAB<sup>®</sup> (version R2020a), following a procedure reported by Tagliaferro et al. [40].

Thermogravimetric analysis (TGA) analysis of hemp fibers and hurds was run using Netzsch TG 209F1 Libra in N<sub>2</sub> flux (20 mL/min) with a temperature ramp of 10 °C/min from 30 to 800 °C and a 30 min final stage in air flux (20 mL/min) for the evaluation of ash content.

For tensile and flexural testing, an MTS Criterion Model 43 universal testing machine (MTS Systems Corporation, Eden Prairie, MN, USA) equipped with a 5 kN load cell was

used. The experiments were performed at a crosshead velocity of 2 and 5 mm/min<sup>-1</sup> for tensile and flexural tests, respectively. The international standards used as reference were ISO 527-2 [38] and ISO 178 [39].

#### 2.2.4. Composite Characterization

Due to the different nature of the tests, multiple types of specimens were manufactured: Dog bone-shaped specimens were produced for the tensile test according to BS EN ISO 527-2:2012, while bar specimens were used for the flexural test according to BS EN ISO 178:2019. The fracture surface of tensile samples was observed using a field-emission scanning electron microscope (FE-SEM, Zeiss SupraTM40, Oberkochen, Germany). These analyses were also performed to investigate the composite microstructure, the distribution of filler particles, and their interfacial bonding with the polymer matrix, as well as to identify failure mechanisms and processing defects.

### 3. Results and Discussion

#### 3.1. Filler Characterization

A preliminary characterization of both hemp fibers and hurds was carried out using TGA analysis, and the main components are shown in Table 1.

**Table 1.** Analysis of the main components of both hemp fibers and hemp hurds.

	Moisture (wt.%)	Hemicellulose (wt.%)	Cellulose (wt.%)	Lignin (wt.%)	Ash (wt.%)
Hemp fibers	5.3	5.4	55.5	32.3	1.5
Hemp hurds	3.5	12.5	43.4	38.5	2.1

As reported by Bartoli et al. [41], both hemp fibers and hemp hurds show the characteristic mass loss associated with hemicellulose (276 °C), cellulose (348 °C), and lignin (above 457 °C) (see Supporting Information Figure S1). The hemp fibers contain a higher cellulose content of up to 55.5 wt.%, compared with 43.4 wt.% for hemp hurds, and lignin and hemicellulose are more abundant in the hurds. For both materials, the ash contents are quite low, ranging from 1.5 up to 2.1 wt.%

The density of both hemp hurds and hemp fibers was measured, resulting in 0.516 g/cm<sup>3</sup> and 0.177 g/cm<sup>3</sup>, respectively.

FESEM captures of hemp fibers and hemp hurds are shown in Figure 1.

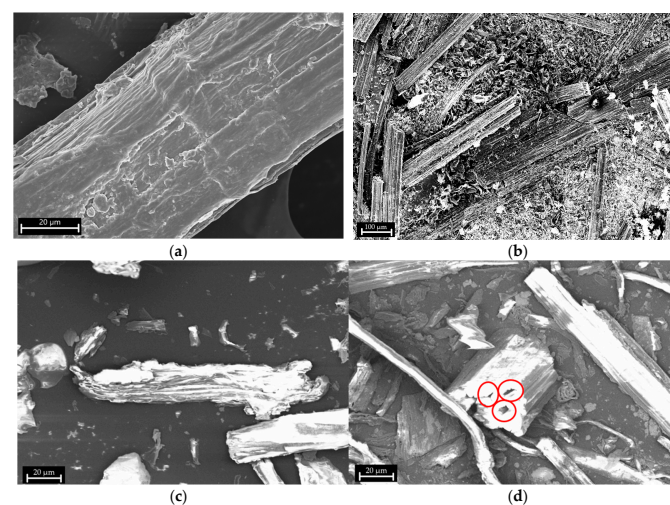


**Figure 1.** FESEM images of hemp fibers (a) and hemp hurds (b) as received, and hemp fibers (c) and hemp hurds (d) after pyrolysis.

As shown in Figure 1a,b, the microscopic morphology of both hemp fibers and hemp hurds is quite similar, showing fibrous structures with an average diameter of up to 18  $\mu\text{m}$ . Interestingly, the surface of hemp hurds is considerably rougher compared to fibers, showing the presence of longitudinal channels [42].

The FESEM images of hemp fibers treated at 400  $^{\circ}\text{C}$  show that the fibers retain their original structure despite the treatment. This structural preservation is significant, as it suggests the robustness of the hemp fibers under demanding thermal conditions. In contrast, the hemp hurds exhibit cracks and tunnels (circled in red in Figure 1), indicating a porous structure after treatment. This porosity in the hemp hurds is likely a result of the decomposition of hemicellulose and lignin, which bind the cellulose fibers together. The structural difference between the hemp fibers and hemp hurds highlights their different responses to thermal treatment, with hemp fibers retaining their integrity, while the hemp hurds become porous. The retention of the integrity is important, as it suggests that the hemp fibers are robust under demanding thermal conditions. In contrast, the hemp hurds show cracks and tunnels, indicating they develop a porous structure after treatment.

The treated fibers largely keep their primary morphology, consistent with what Kabir et al. [13] reported. They described hemp fibers as consisting of cellulose microfibrils surrounded by non-cellulosic components like hemicellulose and lignin. The cracks observed on the fiber surfaces are in line with thermal degradation processes, where the difference in thermal expansion and contraction creates such microstructural features.

Bartoli et al. [6] noted that during pyrolytic treatments, the temperature gradient and the release of volatile organic matter can lead to a partial detachment of the fiber's external parts and the appearance of cracks on the inner sections. This explanation aligns with the observations in the FESEM captures, where cracks appear as a result of the internal stresses and material shrinkage during heating.

Another notable observation is the presence of channels in between the fibers of hemp and in the hemp hurds. These channels are likely a result of the decomposition of the hemicellulose and lignin, which initially holds the fibers together.

As Gauri et al. [14] explained, hemp fibers are multicellular, with elementary fibers bonded by pectin and lignin. During high-temperature treatment, the degradation of these bonding materials causes the fibers to separate, forming inter-fiber channels.

Additionally, the EDX analysis reported in the Table 2 shows an increase in carbon (C) content in the treated fibers compared to the untreated biomass, with a decrease in the O/C ratio. This is significant, as it indicates a higher degree of carbonization in the treated fibers, which is consistent with the breakdown of oxygen-containing groups such as hemicellulose and lignin. The reduction in the O/C ratio suggests a relative increase in carbon content due to the loss of oxygen-containing compounds, resulting in the formation of a more carbon-rich and thermally stable material. This is important for understanding the thermal stability and potential applications of hemp fibers and hemp hurds in various industrial processes.

**Table 2.** EDX of hemp fibers and hemp hurds.

	Elemental Composition (wt.%)	
	C	O
Hemp fibers	67	33
Hemp hurds	74	26

Figure 2 shows the Raman spectra of hemp fibers and hemp hurds. Two main peaks are identified (Table 3): the G peak, located in the 1580–1590  $\text{cm}^{-1}$  range, and the D peak, between 1330  $\text{cm}^{-1}$  and 1370  $\text{cm}^{-1}$ . The  $I_D/I_G$  ratio for hemp fibers is 2.1 and for hemp hurds is 1.8. Their Raman spectra show well-resolved D and G regions, suggesting a disorganized carbonaceous structure [43]. This can be attributed to the complex, heterogeneous nature of the biomass precursors. During pyrolysis, the breakdown of complex organic

molecules produces a carbonaceous material with many defects, leading to a higher D peak intensity. This is supported by the small size of the in-plane graphitic cluster diameter ( $L_a = 18 \text{ \AA}$ ), calculated according to Tuinstra and Koenig [44]. In materials with a high degree of graphitization,  $L_a$  would be significantly larger. The small  $L_a$  values indicate that the carbon atoms are arranged in small graphitic domains, interrupted by numerous defects and amorphous regions.

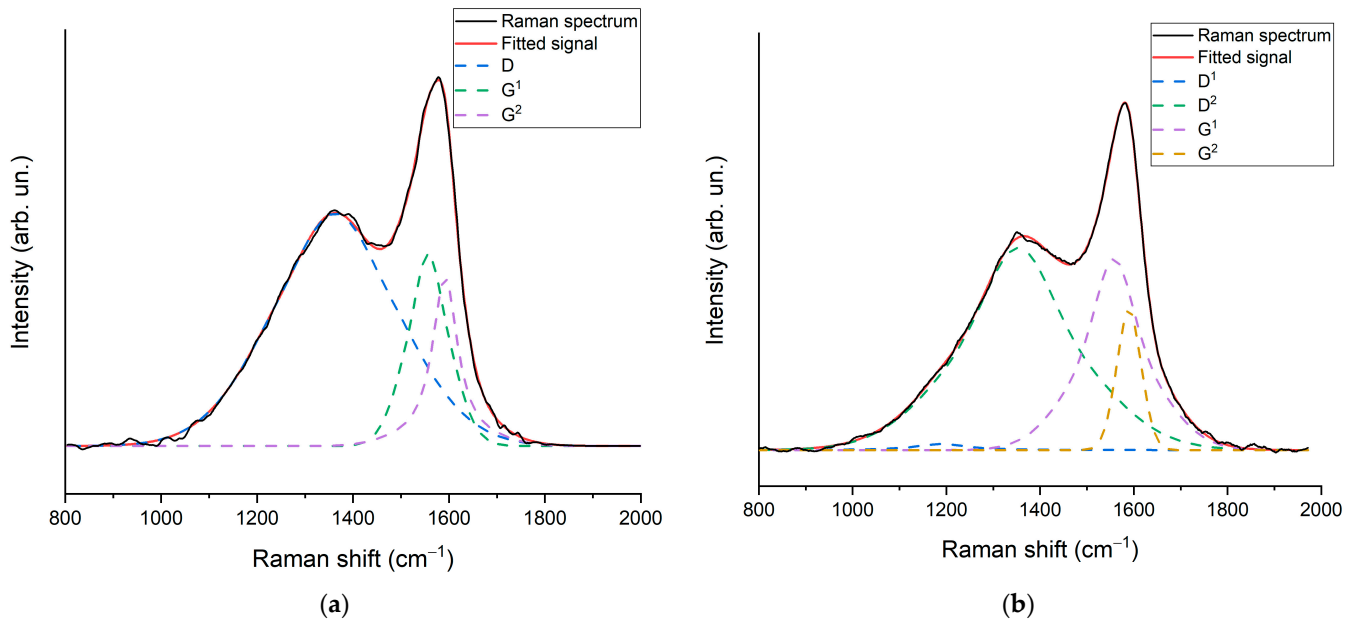


**Figure 2.** Raman spectra of hemp fibers (a) and hemp hurds (b).

**Table 3.** Raman peaks,  $I_D/I_G$  ratio, and  $L_a$  of hemp and hemp hurds.

	D Peak Raman Shift ( $\text{cm}^{-1}$ )	G Peak Raman Shift ( $\text{cm}^{-1}$ )	$I_D/I_G$	$L_a$ ( $\text{\AA}$ )
Hemp fibers	1366	1583	2.1	19
Hemp hurds	1338	1587	1.8	18

Increasing the treatment temperature from  $400 \text{ }^\circ\text{C}$  to  $550 \text{ }^\circ\text{C}$  promotes further conversion of the organic material into a more ordered carbon structure. At lower temperatures (like  $400 \text{ }^\circ\text{C}$ ), the material may still contain a significant amount of organic components and be less graphitized, leading to a higher  $I_D/I_G$  ratio. At higher temperatures (like  $550 \text{ }^\circ\text{C}$ ), the material moves closer to a more graphitic structure, decreasing the number of defects and lowering the  $I_D/I_G$  ratio.

### 3.2. Composite Characterization

In this study, the mechanical properties of composites made from hemp fibers, hemp hurds, and epoxy resin with various filler percentages and different ratios between hemp and hemp hurds were evaluated (Tables 4–11). Tensile tests were conducted to assess the elastic modulus, ultimate tensile strength (UTS), elongation at break, and toughness of the various samples.

**Table 4.** Tensile properties and Spearman’s coefficient of hemp hurd composites.

Tensile Test	Elastic Modulus (GPa)	UTS (MPa)	Elongation at Break (%)	Toughness (MJ/m <sup>3</sup> )
Epoxy	0.5 ± 0.1	10.2 ± 0.7	8.4 ± 2.6	0.73 ± 0.25
Hemp hurds 1 wt.%	0.4 ± 0.1	8.4 ± 0.1	11.3 ± 0.1	0.79 ± 0.08
Hemp hurds 3 wt.%	0.6 ± 0.1	10.5 ± 0.1	6.0 ± 1.6	0.53 ± 0.16
Hemp hurds 5 wt.%	0.2 ± 0.1	10.4 ± 0.5	6.5 ± 0.3	0.58 ± 0.05
Hemp hurds 10 wt.%	0.7 ± 0.1	10.3 ± 1.0	4.3 ± 0.7	0.35 ± 0.09
ρ	0.909	0.303	−0.865	−0.865

**Table 5.** Tensile properties and Spearman’s coefficient of hemp fiber composites.

Tensile Test	Elastic Modulus (GPa)	UTS (MPa)	Elongation at Break (%)	Toughness (MJ/m <sup>3</sup> )
Epoxy	0.5 ± 0.1	10.2 ± 0.7	8.4 ± 2.6	0.73 ± 0.25
Hemp fibers 1 wt.%	0.5 ± 0.1	11.9 ± 0.1	8.2 ± 0.5	0.82 ± 0.02
Hemp fibers 3 wt.%	0.2 ± 0.1	8.9 ± 0.3	12.3 ± 2.0	0.83 ± 0.13
ρ	−0.632	−0.632	0.743	0.287

**Table 6.** Tensile properties and Spearman’s coefficient of 1:1 hemp hurd-to-hemp fiber ratio composites.

Tensile Test	Elastic Modulus (GPa)	UTS (MPa)	Elongation at Break (%)	Toughness (MJ/m <sup>3</sup> )
Epoxy	0.5 ± 0.1	10.2 ± 0.7	8.4 ± 2.6	0.73 ± 0.25
1 wt.% 1:1	1.0 ± 0.1	19.6 ± 1.2	5.9 ± 0.4	1.01 ± 0.08
3 wt.% 1:1	0.9 ± 0.1	19.7 ± 0.4	5.8 ± 1.1	0.95 ± 0.21
5 wt.% 1:1	1.1 ± 0.1	21.0 ± 1.2	3.7 ± 0.3	0.61 ± 0.09
10 wt.% 1:1	0.7 ± 0.1	11.4 ± 0.9	3.3 ± 0.2	0.29 ± 0.02
ρ	−0.310	−0.291	−0.937	−0.867

**Table 7.** Tensile properties and Spearman’s coefficient of 3:1 hemp hurd-to-hemp fiber ratio composites.

Tensile Test	Elastic Modulus (GPa)	UTS (MPa)	Elongation at Break (%)	Toughness (MJ/m <sup>3</sup> )
Epoxy	0.5 ± 0.1	10.2 ± 0.7	8.4 ± 2.6	0.73 ± 0.25
1 wt.% 3:1	0.9 ± 0.1	17.5 ± 0.8	4.4 ± 1.2	0.70 ± 0.21
3 wt.% 3:1	0.8 ± 0.1	16.3 ± 1.6	4.3 ± 0.3	0.53 ± 0.08
5 wt.% 3:1	1.0 ± 0.1	18.5 ± 1.2	3.2 ± 0.3	0.43 ± 0.06
10 wt.% 3:1	1.3 ± 0.1	19.8 ± 0.4	2.2 ± 0.1	0.29 ± 0.01
ρ	0.843	0.775	−0.836	−0.659

**Table 8.** Flexural properties and Spearman’s coefficient of hemp hurd composites.

Flexural Test	Elastic Modulus (GPa)	Maximum Flexural Strength (MPa)	Elongation at Break (%)
Epoxy	0.3 ± 0.1	10.6 ± 0.3	-
Hemp hurds 1 wt.%	0.1 ± 0.1	5.6 ± 0.1	-
Hemp hurds 3 wt.%	0.3 ± 0.1	10.2 ± 0.7	-
Hemp hurds 5 wt.%	0.4 ± 0.1	12.9 ± 1.2	-
Hemp hurds 10 wt.%	0.4 ± 0.1	12.4 ± 0.1	-
ρ	0.812	0.689	-

**Table 9.** Flexural properties and Spearman’s coefficient of hemp fiber composites.

Flexural Test	Elastic Modulus (GPa)	Maximum Flexural Strength (MPa)	Elongation at Break (%)
Epoxy	0.3 ± 0.1	10.6 ± 0.3	-
Hemp fibers 1 wt.%	0.3 ± 0.1	12.3 ± 0.8	-
Hemp fibers 3 wt.%	0.1 ± 0.1	5.5 ± 1.3	-
ρ	−0.478	−0.773	-

**Table 10.** Flexural properties and Spearman’s coefficient of 1:1 hemp hurd-to-hemp fiber ratio composites.

Flexural Test	Elastic Modulus (GPa)	Maximum Flexural Strength (MPa)	Elongation at Break (%)
Epoxy	0.3 ± 0.1	10.6 ± 0.3	-
1 wt.% 1:1	1.3 ± 0.1	34.4 ± 2.1	6.7 ± 0.9
3 wt.% 1:1	1.4 ± 0.1	36.1 ± 0.8	7.6 ± 0.8
5 wt.% 1:1	1.1 ± 0.1	30.4 ± 0.3	6.7 ± 0.1
10 wt.% 1:1	0.7 ± 0.1	19.6 ± 0.4	7.1 ± 0.1
ρ	−0.801	−0.773	-

**Table 11.** Flexural properties and Spearman’s coefficient of 3:1 hemp hurd-to-hemp fiber ratio composites.

Flexural Test	Elastic Modulus (GPa)	Maximum Flexural Strength (MPa)	Elongation at Break (%)
Epoxy	0.3 ± 0.1	10.6 ± 0.3	-
1 wt.% 3:1	1.6 ± 0.1	43.2 ± 1.0	8.4 ± 0.7
3 wt.% 3:1	1.3 ± 0.1	34.3 ± 2.1	8.1 ± 1.3
5 wt.% 3:1	1.2 ± 0.2	33.3 ± 5.7	7.4 ± 2.3
10 wt.% 3:1	1.5 ± 0.1	36.4 ± 1.1	4.8 ± 0.3
ρ	−0.801	−0.773	-

The Spearman correlation coefficient, denoted as ρ, was calculated to analyze the relationships between the elastic modulus, maximum stress, elongation at break, and fracture toughness under both tensile and flexural stress. This coefficient measures the

strength and direction of the association between two ranked variables, evaluating how well their relationship can be described by a monotonic function. Unlike Pearson’s correlation coefficient, which assesses linear relationships, Spearman’s coefficient can also capture nonlinear associations.

Most of the Spearman correlation coefficient values are above 0.6, indicating a strong correlation among the data. In general,  $\rho$  values can be interpreted as follows: (i) strong correlation:  $\rho > 0.6$ , suggesting a reliable relationship between variables; (ii) moderately strong correlation:  $\rho$  between 0.4 and 0.6, indicating a moderate association; (iii) weak or unclear correlation:  $\rho < 0.4$ , showing little to no clear relationship between the variables.

However, in the flexural tests, the elastic modulus of hemp hurds are shown to have a value of 0.478, suggesting only a moderate correlation. In the tensile tests, the elastic modulus and UTS for the 1:1 ratio, the toughness of the hemp fibers, and the UTS of hemp hurds are shown to have values below 0.4, indicating a weak or unclear correlation in these data.

Figures 3–5 shows the mechanical performance of epoxy composites filled with hemp hurds and hemp fibers across different ratios and filler loadings. The pure epoxy serves as a baseline, characterized by moderate stiffness (Young’s modulus of  $0.5 \pm 0.1$  GPa), strength (UTS of  $10.2 \pm 0.7$  MPa), high elongation at break ( $8.4 \pm 2.6\%$ ), and relatively high toughness ( $0.73 \pm 0.25$  MJ/m<sup>3</sup>).

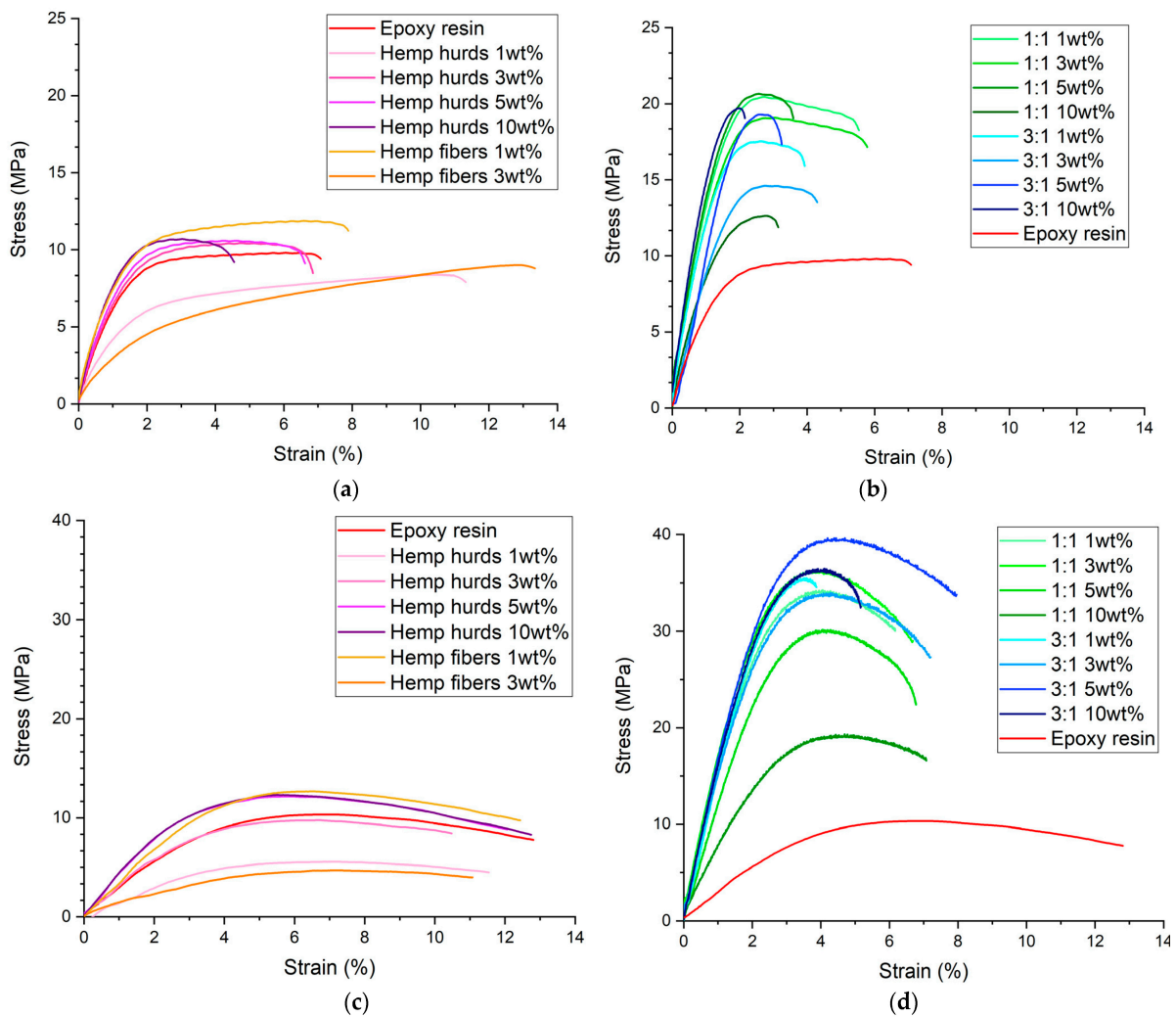


Figure 3. Stress–strain curves obtained from tensile tests (a,b) and flexural tests (c,d).

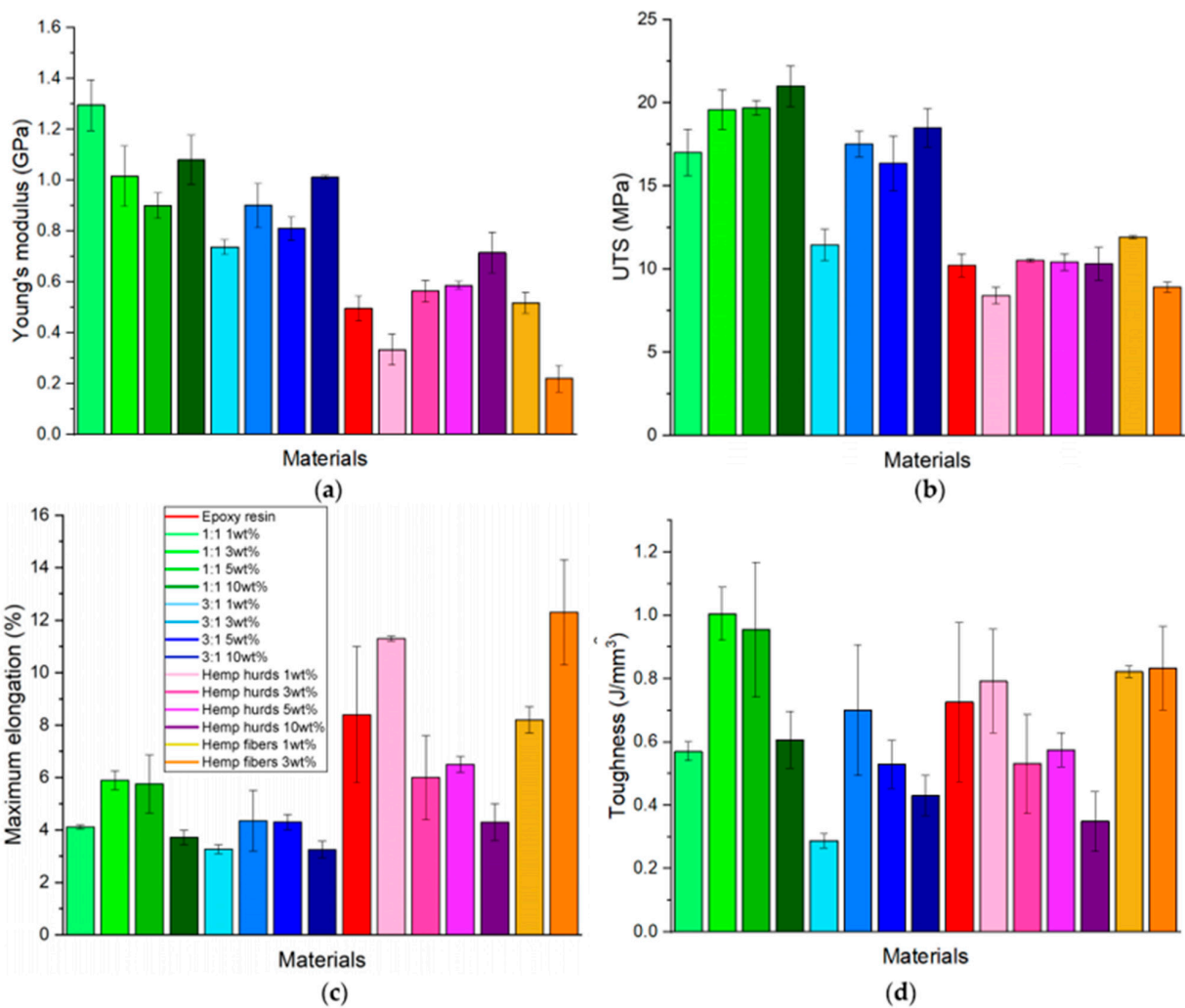


Figure 4. Summary of mechanical properties of composites: Young’s modulus (a), UTS (b), elongation at break (c), and toughness (d).

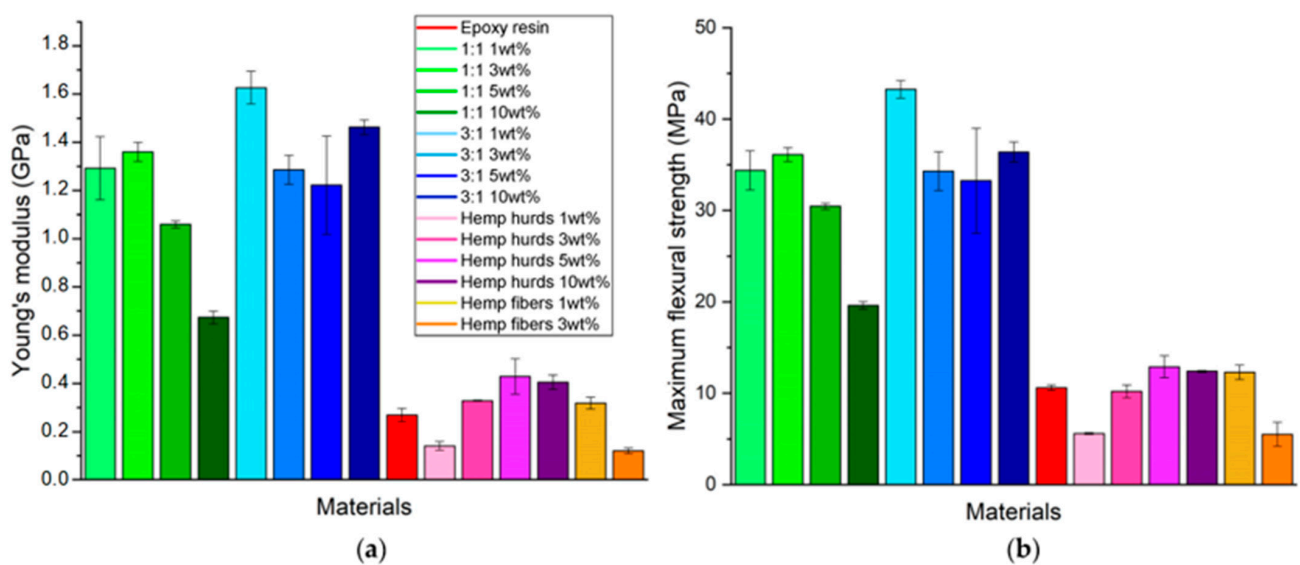


Figure 5. Summary of flexural properties of epoxy composites: flexural modulus (a) and maximum stress (b).

When hemp hurds are introduced into the epoxy matrix at varying concentrations, a complex relationship between the filler content and mechanical properties emerges. At lower concentrations, hemp hurds exhibit a reinforcing effect, particularly in terms of stiffness. For instance, at 3 wt.% of hemp hurds, the Young's modulus increases to  $0.6 \pm 0.1$  GPa, a 20% improvement over the pure epoxy. This increase suggests an effective stress transfer between the epoxy matrix and the hurds. However, UTS does not show a noticeable increase, peaking at  $10.5 \pm 0.1$  MPa (3 wt.%). This suggests that while the composite becomes stiffer, its tensile strength does not experience the same level of enhancement, possibly due to the intrinsic brittleness of the hurds or limited filler–matrix bonding. As the filler loading is increased to 10 wt.%, the composite's Young's modulus continues to improve slightly, reaching  $0.7 \pm 0.1$  GPa, but the UTS decreases slightly to  $10.3 \pm 1$  MPa. This suggests that strength decreases with higher amounts of hurds, likely due to agglomeration of the hurd particles at higher loadings. The decrement in tensile strength despite the increased stiffness could be attributed to weaker interfacial adhesion between the filler and the matrix, which results in stress concentration points that promote premature failure. The use of higher filler loadings may not sufficiently wet the hurds, leading to poor stress distribution and decreased composite integrity. The elongation at break and toughness show more drastic reductions as the filler concentration increases. The composite exhibits an elongation of  $11.3 \pm 0.1\%$ , which is significantly higher than that of the pure epoxy, suggesting improved ductility at very low filler loadings using a loading of 1 wt.% hurds. However, this behavior sharply changes with higher filler contents. For example, at 10 wt.%, elongation drops to  $4.3 \pm 0.7\%$ , marking a substantial reduction in the material's capacity to deform plastically. This decrease in elongation is likely due to the increased stiffness from the hurds, which introduces brittleness into the composite as the polymer matrix's ability to absorb strain decreases. Similarly, toughness follows this trend, dropping from  $0.79 \pm 0.16$  MJ/m<sup>3</sup> at 1 wt.% to  $0.35 \pm 0.09$  MJ/m<sup>3</sup> at 10 wt.%. This suggests that while the material becomes stronger and stiffer at higher hurd loadings, its ability to absorb energy before failure significantly decreases, highlighting the tradeoff between stiffness and toughness that often occurs in fiber-reinforced composites.

Hemp fibers typically provide higher mechanical reinforcement than hurds due to their higher aspect ratio and superior tensile properties. This is reflected in the mechanical performance of the composites. At 1 wt.% of hemp fibers, the Young's modulus reaches  $0.5 \pm 0.1$  GPa, similar to neat epoxy, but the UTS is significantly higher, at  $11.9 \pm 0.1$  MPa. The ability of hemp fibers to reinforce the matrix more effectively than hurds, even at low filler contents, points to their better stress transfer capabilities. The increase in UTS and the marginal improvement in elongation at break ( $8.2 \pm 0.5\%$ ) suggest that the fibers contribute to an overall tougher and more ductile composite at low loadings. However, at 3 wt.% hemp fibers, there is a noticeable reduction in the Young's modulus to  $0.2 \pm 0.1$  GPa, while the elongation at break increases to  $12.3 \pm 2.0\%$ . This unexpected reduction in stiffness, paired with an increase in elongation, might suggest poor dispersion of the fibers at this concentration or a possible fiber pullout phenomenon, where the fibers do not fully adhere to the matrix under stress. The fact that toughness remains fairly high, at  $0.83 \pm 0.13$  MJ/m<sup>3</sup>, suggests that although the composite becomes less stiff, it retains its ability to absorb energy, benefiting from the ductility imparted by the fibers.

The hybrid composites, incorporating both hurds and fibers in different ratios (1:1 and 3:1), demonstrate an even more complex interaction between stiffness, strength, ductility, and toughness. For the 1:1 ratio of hurds to fibers, the stiffness of the composite sees a significant enhancement, with the Young's modulus peaking at  $1.1 \pm 0.1$  GPa at 5 wt.% filler loading. This is a 120% increase over neat epoxy, showcasing the synergistic effect of combining fibers and hurds. The fibers provide tensile reinforcement, while the hurds contribute to the overall stiffness. At 10 wt.%, the modulus drops to  $0.7 \pm 0.1$  GPa, indicating that beyond a certain filler content, the reinforcing effect is decreased. This reduction can be attributed to the poor dispersion of fillers and possible agglomeration, which reduces the effective load-bearing capacity of the matrix. In terms of UTS, the hybrid composites exhibit

their highest strength at 5 wt.% filler loading, with a value of  $21.0 \pm 1.2$  MPa, a twofold increase with respect to neat epoxy. This suggests that the combination of hurds and fibers, when well dispersed, significantly improves the composite's ability to resist tensile loads. However, at higher filler loadings (10 wt.%), the UTS drops sharply to  $11.4 \pm 0.9$  MPa, indicating a loss of strength that can be attributed to poor bonding between the matrix and filler, and the inability of the resin to fully wet the fillers. Elongation at break and toughness follow a downward trend as the filler content increases. At 1 wt.%, the composite exhibits a relatively high elongation of  $5.9 \pm 0.4\%$  and toughness of  $1.01 \pm 0.08$  MJ/m<sup>3</sup>, suggesting good ductility and energy absorption. However, as the filler content increases to 10 wt.%, elongation drops to  $3.3 \pm 0.2\%$  and toughness to  $0.29 \pm 0.02$  MJ/m<sup>3</sup>. This reduction reflects the increased brittleness of the material, as the higher filler content leads to embrittlement, reducing the composite's ability to deform plastically and absorb energy.

For the 3:1 hurd-to-fiber ratio, the trends are somewhat similar, but with subtle differences. The Young's modulus peaks at  $1.3 \pm 0.1$  GPa at 10 wt.% filler content, suggesting that a higher hurd content leads to a stiffer composite. The UTS also remains relatively high, peaking at  $19.8 \pm 0.4$  MPa, indicating that the higher hurd content contributes to strength. However, the elongation at break is significantly lower, at  $2.2 \pm 0.1\%$ , reflecting the increased brittleness of the material at a higher hurd content. Similarly, toughness decreases to  $0.29 \pm 0.01$  MJ/m<sup>3</sup>, suggesting that while the composite becomes stronger and stiffer, its ability to absorb energy before failure is severely compromised.

The flexural test results shown in Figure 5 illustrate the influence of different hemp filler concentrations on the mechanical properties of epoxy composites. Pure epoxy exhibits an elastic modulus of  $0.3 \pm 0.1$  GPa and a maximum flexural strength of  $10.6 \pm 0.3$  MPa, showcasing its relatively moderate stiffness and strength and suggesting a brittle nature.

Incorporating hemp hurds into the epoxy matrix shows variable effects on flexural properties. At a 1 wt.% concentration of hemp hurds, the elastic modulus significantly drops to  $0.1 \pm 0.1$  GPa, and the maximum flexural strength also decreases to  $5.6 \pm 0.1$  MPa, suggesting that this low filler concentration fails to effectively reinforce the epoxy. However, as the concentration of hemp hurds increases to 5 wt.%, both the elastic modulus and the maximum flexural strength improve to  $0.4 \pm 0.1$  GPa and  $12.9 \pm 1.2$  MPa, respectively. This increase highlights the positive impact of adding more filler, enhancing the material's load-bearing capacity due to the magnification of interaction between the matrix and the filler over filler–filler ones using a loading of 10 wt.%, where the elastic modulus remains at  $0.4 \pm 0.1$  GPa. Interestingly, the maximum flexural strength slightly decreases to  $12.4 \pm 0.1$  MPa, indicating a potential plateau in mechanical performance. This could be attributed to insufficient bonding or agglomeration of the hemp hurds, which might disrupt effective stress distribution within the composite.

For hemp fibers, the results reveal a different reinforcement pattern. The elastic modulus is  $0.3 \pm 0.1$  GPa and the maximum flexural strength is  $12.3 \pm 0.8$  MPa at 1 wt.%, reflecting a relatively good improvement compared to pure epoxy. However, when the concentration rises to 3 wt.%, both properties drop to an elastic modulus of  $0.1 \pm 0.1$  GPa and a maximum flexural strength of  $5.5 \pm 1.3$  MPa, suggesting that higher fiber content leads to poorer interaction with the matrix, possibly due to inadequate wetting or dispersion.

Hybrid composites, particularly those with a 1:1 ratio of hemp hurds to fibers, demonstrate significantly enhanced mechanical properties. Using a filler loading of 1 wt.%, the elastic modulus reaches  $1.3 \pm 0.1$  GPa, while the maximum flexural strength improves dramatically to  $34.4 \pm 2.1$  MPa. This significant increase underscores the effectiveness of combining hurds and fibers to achieve better mechanical performance, likely due to improved load transfer mechanisms within the matrix. Further increasing the concentration to 3 wt.% yields an elastic modulus of  $1.4 \pm 0.1$  GPa and a UTS of  $36.1 \pm 0.8$  MPa, reflecting sustained reinforcement from the hybrid approach.

The elastic modulus decreases to  $0.7 \pm 0.1$  GPa and maximum flexural strength drops to  $19.6 \pm 0.4$  MPa, indicating a decline in mechanical performance due to potential overloading, which can compromise the integrity of the composite through agglomeration

and insufficient bonding between the matrix and the fillers due to the ratio between the hemp hurds and hemp fibers for loading of up to 10 wt.% [45].

For the hybrid system with a 3:1 ratio of hurds to fibers, the results show improved strength, particularly at 1 wt.%, where the elastic modulus peaks at  $1.6 \pm 0.1$  GPa and maximum flexural strength at  $43.2 \pm 1.0$  MPa, showcasing the exceptional reinforcement capabilities of this combination.

The fracture mechanism observed in the composites is primarily brittle, with some regions of ductile failure (Figure 6a,b). Comparatively, the ductility is greater at low filler concentration, as revealed by the more extended plastic deformation region on the fracture surface (Figure 6a). This means that a greater amount of energy is absorbed before failure, resulting in higher elongation-at-break values with respect to composites with high filler content, which typically exhibit a much flatter fracture surface (Figure 6b). At higher magnifications, detailed observations of the filler particles can be made, as shown in Figure 6c,d, showing two different scenarios. In the first scenario, the filler particle undergoes partial decohesion at the interface with the matrix (yellow arrows in Figure 6c), indicating poor adhesion between the filler particle and the matrix. This weak interfacial bond prevents the effective transfer of load to the reinforcing phase, limiting the contribution of the filler to the overall increase in Young's modulus [46]. These weak points can act as crack initiation sites at the interface between the epoxy matrix and the filler, with cracks propagating through the matrix, causing plastic deformation of the polymer. In the second scenario, the adhesion between the filler and the matrix is strong. However, cracks initiate within the filler itself, particularly from the tunnels and cracks previously observed in the hemp hurds and highlighted by the red arrow in Figure 6d.

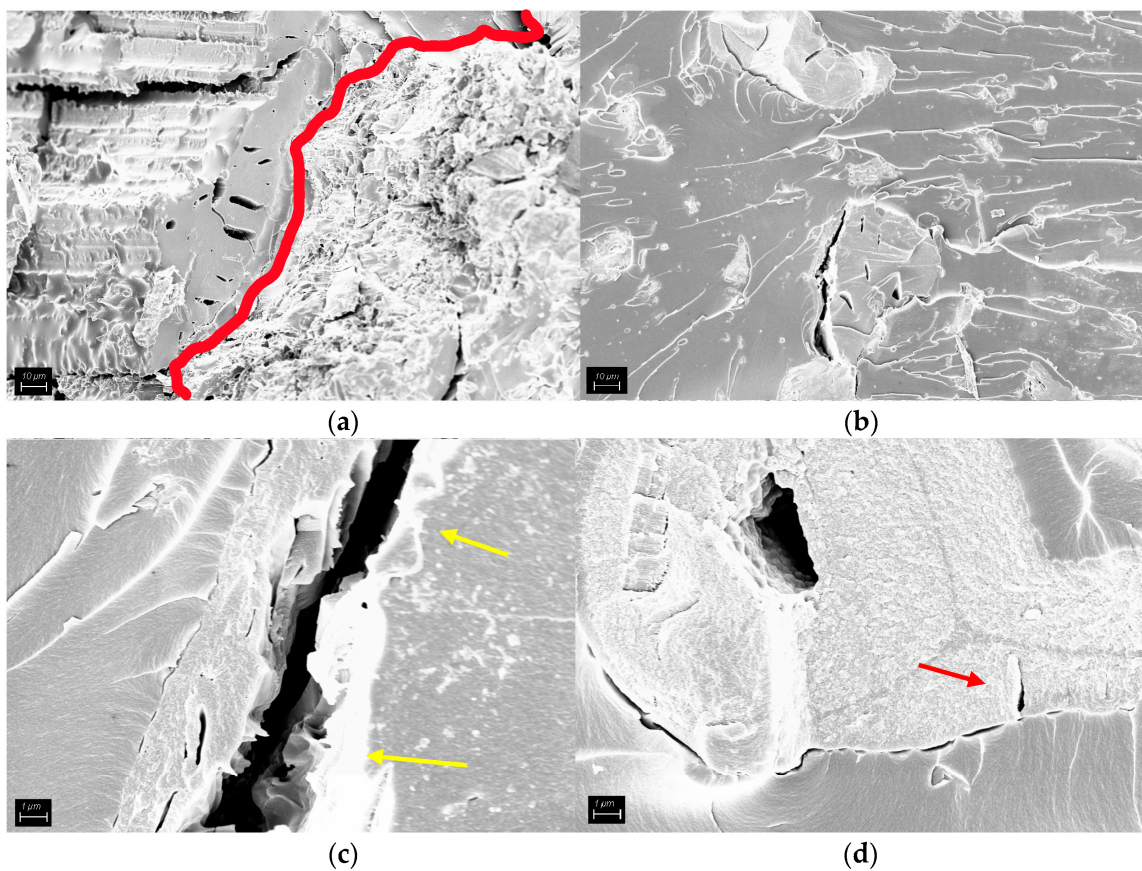


**Figure 6.** FE-SEM images of the fracture surfaces of the composites. Fracture mechanism is primarily brittle, with some regions of ductile failure (a,b); decohesion between filler and matrix (c) and initiation of cracks within the filler itself (d).

As the crack propagates, it causes detachment between the filler and the matrix, further contributing to the failure of the composite.

#### 4. Conclusions

This study has systematically evaluated the mechanical properties of epoxy resin composites reinforced with different concentrations and ratios of hemp fibers and hemp hurds.

The FESEM images show that hemp fibers maintain their original structure even after high-temperature treatment, whereas hemp hurds become porous due to the decomposition of hemicellulose and lignin. This structural integrity of hemp fibers under thermal conditions suggests their robustness, making them suitable for reinforcing composites. In contrast, the porosity observed in hemp hurds could potentially enhance certain properties, such as toughness, by allowing for better energy absorption.

In conclusion, the tensile and flexural properties of epoxy composites reinforced with hemp hurds and hemp fibers demonstrate notable improvements, particularly at lower filler concentrations. The best tensile performance is observed with 1 wt.% hemp fibers, achieving an ultimate tensile strength (UTS) of  $11.9 \pm 0.1$  MPa and toughness of  $0.82 \pm 0.02$  MJ/m<sup>3</sup>. This enhancement is likely due to the effective dispersion of fibers in the epoxy matrix, which promotes better stress transfer between the matrix and the fibers. Hemp fibers have a high aspect ratio and good adhesion to the epoxy, which enables them to carry a greater load when the composite is stressed, leading to higher strength and toughness compared to neat epoxy. Hemp hurds generally improve stiffness but lead to brittleness and reduced toughness at higher loadings. Hemp fibers, on the other hand, offer better tensile reinforcement and maintain ductility at lower concentrations. The hybrid composites demonstrate the most significant improvements in stiffness and strength at moderate filler loadings, but beyond this point, they become increasingly brittle.

In the flexural tests, the highest flexural strength of  $36.1 \pm 0.8$  MPa is achieved with a 1:1 mixture of hemp hurds and fibers at 3 wt.%. This combination likely provides a balance between the rigidity of the hurds and the flexibility of the fibers, improving the composite's ability to resist bending forces. At this optimal ratio, the fibers prevent crack propagation while the hurds contribute to stiffness, leading to an improved flexural modulus of  $1.4 \pm 0.1$  GPa. The lower filler concentrations prevent the agglomeration of particles, ensuring better distribution within the epoxy matrix and maximizing the interfacial bonding, which is essential for achieving high mechanical performance.

These findings underscore the importance of optimizing the filler content and ratio to achieve the desired mechanical properties in epoxy resin composites reinforced with natural fibers.

The present paper illustrates the successful fabrication of composites made with epoxy resin and hemp fibers and hemp hurds, which can be used for semi-structural applications. The automobile industry, followed by the construction and consumer product industries, are the most important sectors that can use hemp-based composites.

**Supplementary Materials:** The following supporting information can be downloaded at: <https://www.mdpi.com/article/10.3390/jcs8110473/s1>, Figure S1: TGA analysis of (a) hemp fibers and (b) hemp hurds (thermograms are reported in black lines, DTG curves are reported in red lines).

**Author Contributions:** Conceptualization, S.Z. and M.B.; methodology, S.Z., G.C. and M.B.; validation, M.B.; formal analysis, S.Z., G.C. and M.B.; investigation, S.Z.; resources, C.R. and A.T.; data curation, S.Z. and M.B.; writing—original draft preparation, S.Z.; writing—review and editing, S.Z., G.C., M.B., C.R. and A.T.; visualization, S.Z.; supervision, M.B., C.R. and A.T. All authors have read and agreed to the published version of the manuscript.

**Funding:** This research received no external funding.

**Data Availability Statement:** The original contributions presented in the study are included in the article/Supplementary Material, further inquiries can be directed to the corresponding authors.

**Conflicts of Interest:** The authors declare no conflicts of interest.

## References

1. Mohanty, A.K.; Vivekanandhan, S.; Pin, J.-M.; Misra, M. Composites from renewable and sustainable resources: Challenges and innovations. *Science* **2018**, *362*, 536–542. [[CrossRef](#)] [[PubMed](#)]
2. Herrera-Franco, P.; Valadez-Gonzalez, A. A study of the mechanical properties of short natural-fiber reinforced composites. *Compos. Part B Eng.* **2005**, *36*, 597–608. [[CrossRef](#)]
3. Piatti, E.; Torsello, D.; Gavello, G.; Ghigo, G.; Gerbaldo, R.; Bartoli, M.; Duraccio, D. Tailoring the Magnetic and Electrical Properties of Epoxy Composites Containing Olive-Derived Biochar through Iron Modification. *Nanomaterials* **2023**, *13*, 2326. [[CrossRef](#)] [[PubMed](#)]
4. Ahmetli, G.; Kocaman, S.; Ozaytekin, I.; Bozkurt, P. Epoxy composites based on inexpensive char filler obtained from plastic waste and natural resources. *Polym. Compos.* **2013**, *34*, 500–509. [[CrossRef](#)]
5. Peças, P.; Carvalho, H.; Salman, H.; Leite, M. Natural fibre composites and their applications: A review. *J. Compos. Sci.* **2018**, *2*, 66. [[CrossRef](#)]
6. Bartoli, M.; Duraccio, D.; Faga, M.G.; Piatti, E.; Torsello, D.; Ghigo, G.; Malucelli, G. Mechanical, electrical, thermal and tribological behavior of epoxy resin composites reinforced with waste hemp-derived carbon fibers. *J. Mater. Sci.* **2022**, *57*, 14861–14876. [[CrossRef](#)]
7. Manaia, J.P.; Manaia, A.T.; Rodrigues, L. Industrial hemp fibers: An overview. *Fibers* **2019**, *7*, 106. [[CrossRef](#)]
8. Ruano, G.; Bellomo, F.; Lopez, G.; Bertuzzi, A.; Nallim, L.; Oller, S. Mechanical behaviour of cementitious composites reinforced with bagasse and hemp fibers. *Constr. Build. Mater.* **2020**, *240*, 117856. [[CrossRef](#)]
9. Ahmed, A.F.; Islam, M.Z.; Mahmud, M.S.; Sarker, M.E.; Islam, M.R. Hemp as a potential raw material toward a sustainable world: A review. *Heliyon* **2022**, *8*, e08753. [[CrossRef](#)]
10. Marrot, L.; Lefeuvre, A.; Pontoire, B.; Bourmaud, A.; Baley, C. Analysis of the hemp fiber mechanical properties and their scattering (Fedora 17). *Ind. Crops Prod.* **2013**, *51*, 317–327. [[CrossRef](#)]
11. Shahzad, A. Hemp fiber and its composites—a review. *J. Compos. Mater.* **2012**, *46*, 973–986. [[CrossRef](#)]
12. Stevulova, N.; Cigasova, J.; Purcz, P.; Schwarzova, I.; Kacik, F.; Geffert, A. Water absorption behavior of hemp hurds composites. *Materials* **2015**, *8*, 2243–2257. [[CrossRef](#)]
13. Chang, B.P.; Rodriguez-Urbe, A.; Mohanty, A.K.; Misra, M. A comprehensive review of renewable and sustainable biosourced carbon through pyrolysis in biocomposites uses: Current development and future opportunity. *Renew. Sustain. Energy Rev.* **2021**, *152*, 111666. [[CrossRef](#)]
14. Henderson, K.; Loreau, M. A model of Sustainable Development Goals: Challenges and opportunities in promoting human well-being and environmental sustainability. *Ecol. Model.* **2023**, *475*, 110164. [[CrossRef](#)]
15. Dissanayake, P.D.; You, S.; Igalavithana, A.D.; Xia, Y.; Bhatnagar, A.; Gupta, S.; Kua, H.W.; Kim, S.; Kwon, J.-H.; Tsang, D.C. Biochar-based adsorbents for carbon dioxide capture: A critical review. *Renew. Sustain. Energy Rev.* **2020**, *119*, 109582. [[CrossRef](#)]
16. Haleem, N.; Khattak, A.; Jamal, Y.; Sajid, M.; Shahzad, Z.; Raza, H. Development of poly vinyl alcohol (PVA) based biochar nanofibers for carbon dioxide (CO<sub>2</sub>) adsorption. *Renew. Sustain. Energy Rev.* **2022**, *157*, 112019. [[CrossRef](#)]
17. Liu, W.-J.; Jiang, H.; Yu, H.-Q. Development of biochar-based functional materials: Toward a sustainable platform carbon material. *Chem. Rev.* **2015**, *115*, 12251–12285. [[CrossRef](#)]
18. Zhang, C.; Khorshidi, H.; Najafi, E.; Ghasemi, M. Fresh, mechanical and microstructural properties of alkali-activated composites incorporating nanomaterials: A comprehensive review. *J. Clean. Prod.* **2023**, *384*, 135390. [[CrossRef](#)]
19. Cordon, H.C.F.; Cagnoni, F.C.; Ferreira, F.F. Comparison of physical and mechanical properties of civil construction plaster and recycled waste gypsum from São Paulo, Brazil. *J. Build. Eng.* **2019**, *22*, 504–512. [[CrossRef](#)]
20. Abbas, M.; Jeon, H.-Y. *Generation, Development and Modifications of Natural Fibers*; BoD—Books on Demand: Norderstedt, Germany, 2020.
21. Patel, R.V.; Yadav, A.; Winczek, J. Physical, mechanical, and thermal properties of natural fiber-reinforced epoxy composites for construction and automotive applications. *Appl. Sci.* **2023**, *13*, 5126. [[CrossRef](#)]
22. Ismail, S.O.; Akpan, E.; Dhakal, H.N. Review on natural plant fibres and their hybrid composites for structural applications: Recent trends and future perspectives. *Compos. Part C Open Access* **2022**, *9*, 100322. [[CrossRef](#)]
23. Syduzzaman, M.; Al Faruque, M.A.; Bilisik, K.; Naebe, M. Plant-based natural fibre reinforced composites: A review on fabrication, properties and applications. *Coatings* **2020**, *10*, 973. [[CrossRef](#)]
24. Pickering, K. *Properties and Performance of Natural-Fibre Composites*; Elsevier: Amsterdam, The Netherlands, 2008.
25. Sun, Z.; Xu, L.; Chen, Z.; Wang, Y.; Tusiime, R.; Cheng, C.; Zhou, S.; Liu, Y.; Yu, M.; Zhang, H. Enhancing the mechanical and thermal properties of epoxy resin via blending with thermoplastic polysulfone. *Polymers* **2019**, *11*, 461. [[CrossRef](#)] [[PubMed](#)]
26. Kerni, L.; Singh, S.; Patnaik, A.; Kumar, N. A review on natural fiber reinforced composites. *Mater. Today Proc.* **2020**, *28*, 1616–1621. [[CrossRef](#)]
27. Haramina, T.; Hadžić, N.; Keran, Z. Epoxy Resin Biocomposites Reinforced with flax and hemp fibers for marine applications. *J. Mar. Sci. Eng.* **2023**, *11*, 382. [[CrossRef](#)]
28. Dahal, R.K.; Acharya, B.; Dutta, A. The Interaction Effect of the Design Parameters on the Water Absorption of the Hemp-Reinforced Biocarbon-Filled Bio-Epoxy Composites. *Int. J. Mol. Sci.* **2023**, *24*, 6093. [[CrossRef](#)]
29. Soni, P.; Sinha, S. Fiber and future: Unleashing the power of industrial hemp waste through epoxy composites. *Polym. Compos.* **2024**, *45*, 413–423. [[CrossRef](#)]

30. Bollino, F.; Giannella, V.; Armentani, E.; Sepe, R. Mechanical behavior of chemically-treated hemp fibers reinforced composites subjected to moisture absorption. *J. Mater. Res. Technol.* **2023**, *22*, 762–775. [[CrossRef](#)]
31. Pickering, K.L.; Efendy, M.A.; Le, T.M. A review of recent developments in natural fibre composites and their mechanical performance. *Compos. Part A Appl. Sci. Manuf.* **2016**, *83*, 98–112. [[CrossRef](#)]
32. Balčiūnas, G.; Vėjelis, S.; Vaitkus, S.; Kairyte, A. Physical properties and structure of composite made by using hemp hurds and different binding materials. *Procedia Eng.* **2013**, *57*, 159–166. [[CrossRef](#)]
33. Cigasova, J.; Stevulova, N.; Junak, J. Properties monitoring of fibrous composites based on hemp hurds with different mean particle size. *Pollack Period.* **2013**, *8*, 41–46. [[CrossRef](#)]
34. Caprino, G.; Carrino, L.; Durante, M.; Langella, A.; Lopresto, V. Low impact behaviour of hemp fibre reinforced epoxy composites. *Compos. Struct.* **2015**, *133*, 892–901. [[CrossRef](#)]
35. Katiyar, J.K.; Sinha, S.K.; Kumar, A. Effects of carbon fillers on the tribological and mechanical properties of an epoxy-based polymer (SU-8). *Tribol.-Mater. Surf. Interfaces* **2016**, *10*, 33–44. [[CrossRef](#)]
36. Mirițoiu, C.M.; Stănescu, M.M.; Burada, C.O.; Bolcu, D.; Pădeanu, A.; Bolcu, A. Comparisons between some composite materials reinforced with hemp fibers. *Mater. Today Proc.* **2019**, *12*, 499–507. [[CrossRef](#)]
37. Bartoli, M.; Giorcelli, M.; Rosso, C.; Rovere, M.; Jagdale, P.; Tagliaferro, A. Influence of commercial biochar fillers on brittleness/ductility of epoxy resin composites. *Appl. Sci.* **2019**, *9*, 3109. [[CrossRef](#)]
38. ISO 527-2:2012; Plastics—Determination of Tensile Properties—Part 2: Test Conditions for Moulding and Extrusion Plastics. Korean Standard Association: Seoul, Republic of Korea, 2013.
39. UNI EN ISO 178:2019; Materie Plastiche—Determinazione Delle Proprietà di Flessione. ISO: Geneva, Switzerland, 2019.
40. Tagliaferro, A.; Rovere, M.; Padovano, E.; Bartoli, M.; Giorcelli, M. Introducing the novel mixed gaussian-lorentzian lineshape in the analysis of the raman signal of biochar. *Nanomaterials* **2020**, *10*, 1748. [[CrossRef](#)]
41. Bartoli, M.; Nasir, M.A.; Jagdale, P.; Passaglia, E.; Spiniello, R.; Rosso, C.; Giorcelli, M.; Rovere, M.; Tagliaferro, A. Influence of pyrolytic thermal history on olive pruning biochar and related epoxy composites mechanical properties. *J. Compos. Mater.* **2020**, *54*, 1863–1873. [[CrossRef](#)]
42. Arizzi, A.; Cultrone, G.; Brümmer, M.; Viles, H. A chemical, morphological and mineralogical study on the interaction between hemp hurds and aerial and natural hydraulic lime particles: Implications for mortar manufacturing. *Constr. Build. Mater.* **2015**, *75*, 375–384. [[CrossRef](#)]
43. Di Maro, M.; Faga, M.G.; Pedraza, R.; Malucelli, G.; Bartoli, M.; Gomez d’Ayala, G.; Duraccio, D. Effect of Hemp Hurd Biochar and Humic Acid on the Flame Retardant and Mechanical Properties of Ethylene Vinyl Acetate. *Polymers* **2023**, *15*, 1411. [[CrossRef](#)]
44. Ferrari, A.; Robertson, J. Interpretation of Raman spectra of disordered and amorphous carbon. *Phys. Rev. B* **2000**, *61*, 14095. [[CrossRef](#)]
45. Dayo, A.Q.; Wang, J.; Wang, A.-R.; Lv, D.; Zegaoui, A.; Derradji, M.; Liu, W.-B. Mechanical and thermal properties of a room temperature curing epoxy resin and related hemp fibers reinforced composites using a novel in-situ generated curing agent. *Mater. Chem. Phys.* **2018**, *203*, 293–301.
46. Neves, A.C.C.; Rohen, L.A.; Mantovani, D.P.; Carvalho, J.P.; Vieira, C.M.F.; Lopes, F.P.; Simonassi, N.T.; da Luz, F.S.; Monteiro, S.N. Comparative mechanical properties between biocomposites of Epoxy and polyester matrices reinforced by hemp fiber. *J. Mater. Res. Technol.* **2020**, *9*, 1296–1304. [[CrossRef](#)]

**Disclaimer/Publisher’s Note:** The statements, opinions and data contained in all publications are solely those of the individual author(s) and contributor(s) and not of MDPI and/or the editor(s). MDPI and/or the editor(s) disclaim responsibility for any injury to people or property resulting from any ideas, methods, instructions or products referred to in the content.